



US Army Corps
of Engineers®

Seepage-Based Factor of Safety Analysis Using 3D Groundwater Simulation Results

*by Hwai-Ping Cheng, Kevin D. Winters,
Stephen M. England, and Ryan E. Pickett*

PURPOSE: The purpose of this Coastal and Hydraulics Engineering Technical Note (CHETN) is to document techniques for computing Factors of Safety (FoS) for seepage-related soil instability of earthen structures, using the simulation results from a 3D, finite-element groundwater model.

BACKGROUND: The FoS analysis has been used widely in geotechnical practice to describe a soil's state versus some critical condition, often associated with engineering failure. It is a simple and reliable supplement to conventional analysis that accommodates the combined effects of the parameters and uncertainties involved in the calculations. Traditional practice for seepage analysis has been to use 2D groundwater models (e.g., SEEP/W (<http://www.geo-slope.com/products/seepw.aspx>) and SEEP2D (<http://www.aquaveo.com/software/gms-seep2d>)), to evaluate issues related to piping and seepage through impoundment structures such as levees, dikes, and dams (Davis et al. 2009). Although the incorporation of variability in model parameters into these FoS analyses helps to account for uncertainties from different sources (Duncan 2000), there remain several inherent limitations in using these 2D cross-section-type models. Several of the limitations associated with 2D modeling can be eliminated through the use of 3D models. For example, 2D models cannot account for variation in topography, geology, sources or sinks, and boundary conditions along the length of the soil structure. If these conditions exist, a 3D model may be needed.

Seepage-Based Factor of Safety. Beginning with a laboratory setup as shown in Figure 1, the stability of the soil may depend on whether the net force at a point X is upward or downward. Suppose the soil matrix is in a hydrostatic condition, then the upward force and the downward force at point X can be expressed as

$$F_{upward}^X = (\Delta H + d_{ponding} + L)\gamma_w \quad (1)$$

$$F_{downward}^X = d_{ponding}\gamma_w + L\gamma_s \quad (2)$$

with the unit weight of the saturated soil (γ_s) defined as

$$\gamma_s = \phi\gamma_w + (1 - \phi)\gamma_{dry} \quad (3)$$

Report Documentation Page			Form Approved OMB No. 0704-0188		
Public reporting burden for the collection of information is estimated to average 1 hour per response, including the time for reviewing instructions, searching existing data sources, gathering and maintaining the data needed, and completing and reviewing the collection of information. Send comments regarding this burden estimate or any other aspect of this collection of information, including suggestions for reducing this burden, to Washington Headquarters Services, Directorate for Information Operations and Reports, 1215 Jefferson Davis Highway, Suite 1204, Arlington VA 22202-4302. Respondents should be aware that notwithstanding any other provision of law, no person shall be subject to a penalty for failing to comply with a collection of information if it does not display a currently valid OMB control number.					
1. REPORT DATE AUG 2014		2. REPORT TYPE		3. DATES COVERED 00-00-2014 to 00-00-2014	
4. TITLE AND SUBTITLE Seepage-Based Factor of Safety Analysis Using 3D Groundwater Simulation Results			5a. CONTRACT NUMBER		
			5b. GRANT NUMBER		
			5c. PROGRAM ELEMENT NUMBER		
6. AUTHOR(S)			5d. PROJECT NUMBER		
			5e. TASK NUMBER		
			5f. WORK UNIT NUMBER		
7. PERFORMING ORGANIZATION NAME(S) AND ADDRESS(ES) ERDC/CHL,3909 Halls Ferry Road,,Vicksburg,MS,39180			8. PERFORMING ORGANIZATION REPORT NUMBER		
9. SPONSORING/MONITORING AGENCY NAME(S) AND ADDRESS(ES)			10. SPONSOR/MONITOR'S ACRONYM(S)		
			11. SPONSOR/MONITOR'S REPORT NUMBER(S)		
12. DISTRIBUTION/AVAILABILITY STATEMENT Approved for public release; distribution unlimited					
13. SUPPLEMENTARY NOTES					
14. ABSTRACT					
15. SUBJECT TERMS					
16. SECURITY CLASSIFICATION OF:			17. LIMITATION OF ABSTRACT Same as Report (SAR)	18. NUMBER OF PAGES 14	19a. NAME OF RESPONSIBLE PERSON
a. REPORT unclassified	b. ABSTRACT unclassified	c. THIS PAGE unclassified			

where ΔH is the difference in head across the soil layer, $d_{ponding}$ is the depth of water above the soil matrix, L is the thickness of the soil matrix, γ_w is the unit weight of water, ϕ is the porosity, and γ_{dry} is the unit weight of the dry soil matrix.

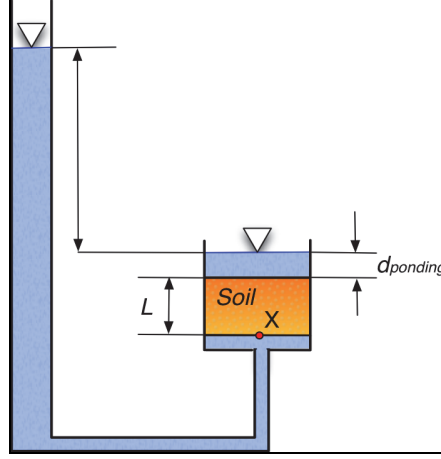


Figure 1. Factor of Safety determination.

Three scenarios regarding the stability of the soil thus exist:

Critical Condition: When $F_{upward}^X = F_{downward}^X$, there results

$$(\Delta H + d_{ponding} + L)\gamma_w = d_{ponding}\gamma_w + L\gamma_s \quad (4)$$

which can be rewritten as

$$\frac{\Delta H}{L} = (1 - \phi) \left(\frac{\gamma_{dry}}{\gamma_w} - 1 \right) = (1 - \phi)(G_s - 1) \quad (5)$$

where G_s is the specific gravity of the soil.

Stable Condition: When $F_{upward}^X < F_{downward}^X$, there results

$$\frac{\Delta H}{L} < (1 - \phi)(G_s - 1) \quad (6)$$

Unstable Condition: When $F_{upward}^X > F_{downward}^X$, there results

$$\frac{\Delta H}{L} > (1 - \phi)(G_s - 1) \quad (7)$$

Therefore, the FoS can be defined as the ratio of the stabilizing downward force to the generally destabilizing upward force applied to the soil. It can be written as

$$FoS = \frac{(1 - \phi)(G_s - 1)}{\left(\frac{\Delta H}{L}\right)} = \frac{i_{cr}}{i_v} \quad (8)$$

where i_{cr} is the critical hydraulic gradient, and i_v is the exit gradient at the point of interest. The critical, stable, and unstable conditions are thus defined as $FoS = 1$, $FoS > 1$, and $FoS < 1$ (or $i_{cr} = i_v$, $i_{cr} > i_v$, and $i_{cr} < i_v$), respectively. Under the critical condition, the vertical effective stress is zero, but under unstable conditions, the potential for movement of soil exists. Due to variability of factors, the critical condition is unlikely to exist. Therefore, an FoS screening criteria > 1 is chosen to distinguish stable and unstable conditions in general practice.

In general, the exit gradient at a point of interest can be computed from the simulated head distribution of a model as explained in Figure 2, where the computational model accounts for boundary conditions, sources/sinks, any overlying material at the point of interest, and the specified ponding depth above the top soil. The aforementioned exit gradient across the soil is assumed to be constant and may be estimated from the values of total head at points X and Y and the vertical distance between the points (i.e., L (Figure 2)). The total heads at X and Y are denoted by H_X and H_Y , respectively, in Equation 9.

$$i_v = \frac{\Delta H}{L} = \frac{H_X - H_Y}{L} \quad (9)$$

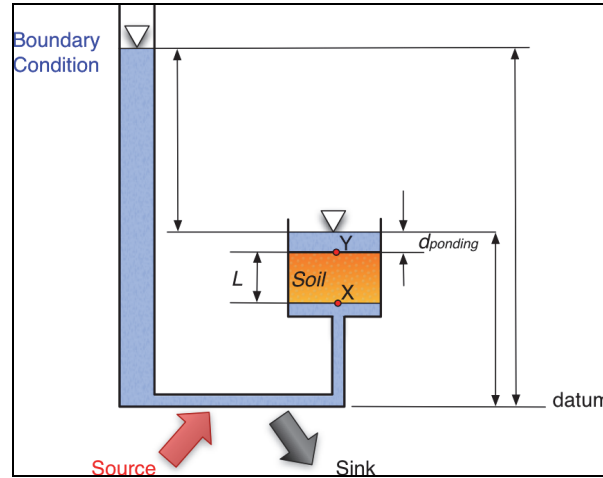


Figure 2. Hydraulic gradient at a point-of-interest computation.

According to the U.S. Army Corps of Engineers (USACE), Jacksonville District Memorandum with the subject *Herbert Hoover Dike Loadings and Factors of Safety for Use in Seepage and Stability Analyses* (U.S. Army Corps of Engineers (USACE), Jacksonville District 2008), the FoS against piping of foundation soils due to under seepage (FoS_{piping}) and the FoS against uplift,

or heave, of blanket materials (FoS_{uplift}) should be calculated for dike-safety evaluation, where FoS_{piping} is for pipeable topsoil (noncohesive soils such as sand) and FoS_{uplift} for nonpipeable topsoil (cohesive soils such as clay and silt). The FoS for pipeable material (i.e., FoS_{piping}) can be computed directly using Equation 8 while FoS_{uplift} for nonpipeable materials can be computed using the following equation:

$$FoS_{uplift} = \frac{i_{cr}}{i_v} = \frac{\left(\frac{\sum_{i=1}^n (\gamma_i - \gamma_w) \Delta z_i}{\gamma_w \sum_{i=1}^n \Delta z_i} \right)}{\frac{\Delta H}{\Delta z}} = \frac{\sum_{i=1}^n (1 - \phi_i) (G_i - 1) \Delta z_i}{\Delta H} \quad (10)$$

where n is the number of soil types included in the nonpipeable layer, ϕ_i is the porosity of the i -th soil type, G_i is the specific gravity of the i -th soil type, and $\Delta z = \sum_{i=1}^n \Delta z_i$ denotes the total thickness of the nonpipeable layer.

Note that Equations 8 and 10 used to compute FoS for piping and uplift are essentially the same. However, the mechanism for initiation is slightly different. Piping can be thought of as a phenomenon where the gradient through the soil is such that movement of individual soil grains is possible, whereas uplift is a condition when the pressure beneath the blanket exceeds the effective weight of the blanket material and water. While piping deals with pipeable materials as sands, uplift considers nonpipeable, low-permeability materials such as clays and may involve multiple materials of different thicknesses. That is, the computation of uplift includes the composite effect of the weight of all the layers, but the piping FoS calculation in a multilayer system would be the minimum value among the layers.

METHODOLOGY FOR FACTOR OF SAFETY COMPUTATION: A computer program, written in Fortran 90, was developed as a postprocessor for the 3D WASH123D groundwater model (Yeh et al. 2006), a finite element computational model that approximates the Richards equation for pressure heads at the nodes of unstructured meshes. The postprocessing utility code computes FoS_{piping} using Equation 8 with the exit gradient defined as

$$i = \frac{H_B - H_A}{d_{AB}} \quad (11)$$

where H_A is the total head at a boundary-face node A, H_B is the total head at a nonboundary-face node B that is associated with node A, and d_{AB} is the distance from node A to node B.

Generally, the distance from node A to node B is close to the thickness of the soil associated with node A divided by the number of element layers used to discretize the material. For instance, if the soil shown in Figure 3 associated with the boundary-face node A is one foot (ft) thick and discretized using a single layer of elements, then the distance from node A to node B should be approximately a foot.

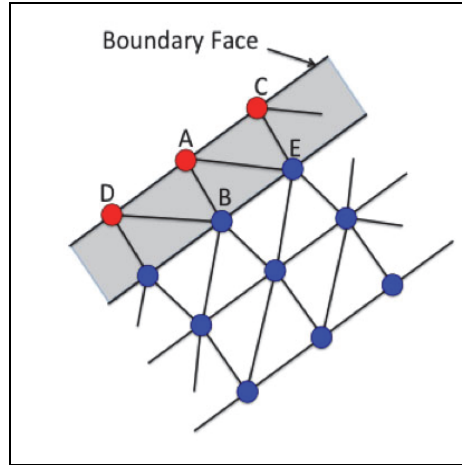


Figure 3. The exit gradient computed at boundary-face node A uses the total heads at nodes A and B and the distance from nodes A to B. The exit gradient may be neither vertical nor horizontal.

The utility code requires the following data as input:

- The mesh of the 3D groundwater model of interest, which includes
 - nodal coordinates and
 - element indices.
- The head distribution over the entire domain of the 3D model (total or pressure head).
- The parameters necessary to compute FoS, which includes
 - specific weight of water,
 - specific weight of soil materials (solids),
 - porosity of soil materials, and
 - FoS screening criteria.

The utility code computes the critical gradient and the FoS value associated with each of the boundary-face nodes of interest. To help the analysis, it also outputs the exit gradient computed at each node of interest.

Computation of Exit Gradient at Unstructured Mesh Nodes. In the preceding, the FoS and the exit gradient were considered only in the vertical direction. O’Leary et al. (2013) provided an overview of the available methods that can be used to evaluate critical horizontal seepage gradients. The angle of internal friction that can be determined in the laboratory by a direct shear test or a triaxial stress test needs to be taken into account when the horizontal FoS is evaluated. Al-Hussaini et al. (1997) proposed to use the following equation to compute critical horizontal gradient:

$$i_{cr}^{horizontal} = i_{cr} \tan \phi \quad (12)$$

where ϕ is the angle of internal friction. The angle of internal friction ranges from 20° (clay) to 48° (gravel with some sand). As a result, the coefficient of internal friction ($\tan \phi$) ranges from 0.364 to 1.11, making the critical gradient either lower or higher than the vertical gradient. While the utility uses Equation 12 to compute the horizontal critical gradient, other methods can also be incorporated into the utility for better estimates.

Due either to the topographical variation or to the discretization of unstructured mesh, the exit gradient computed can be in a direction that is neither vertical nor horizontal (Figure 3). To handle this situation, the utility code computes both vertical FoS and horizontal FoS using the computed head at the nonboundary-face node closest to the boundary-face node of interest. For example, node B is the nonboundary-face node closest to the boundary-face node A in Figure 3. The vertical FoS (i.e., $FoS_{AB}^{vertical}$) and the horizontal FoS (i.e., $FoS_{AB}^{horizontal}$) associated with nodes A and B can thus be computed as

$$FoS_{AB}^{vertical} = \frac{i_{cr}}{i} = \frac{(G_s - 1)}{\left(\frac{H_B - H_A}{d_{AB}} \right)} = \frac{(G_s - 1)d_{AB}}{(H_B - H_A)} \quad (13)$$

$$FoS_{AB}^{horizontal} = \frac{i_{cr}^{horizontal}}{i} = \frac{(G_s - 1) \tan \phi}{\left(\frac{H_B - H_A}{d_{AB}} \right)} = \frac{(G_s - 1)d_{AB}}{(H_B - H_A)} \tan \phi \quad (14)$$

where H_A is the total head at a boundary-face node A, H_B is the total head at a nonboundary-face node B, and d_{AB} is the distance from node A to node B.

With the fact that only the vertical FoS needs to be evaluated when the boundary face is horizontal, and only the horizontal FoS is needed when the boundary face is vertical, the final FoS for a location on a sloped boundary face can be estimated using a simple equation accounting for the contributions from both the vertical FoS and the horizontal FoS as

$$FoS_{piping} = Fos_{AB}^{vertical} \cos \alpha + Fos_{AB}^{horizontal} \sin \alpha \quad (15)$$

where $\cos \alpha = \frac{\Delta z_{AB}}{d_{AB}}$, $\sin \alpha = \frac{\Delta x_{AB}}{d_{AB}}$, and Δz_{AB} and Δx_{AB} are the vertical and the horizontal distances, respectively, between nodes A and B.

To calculate FoS adequately, the nonboundary-face node used should be placed in a location such that the straight line connecting it and the respective boundary-face node is approximately perpendicular to the sloped boundary face. This needs to be taken into account during the development of the computational mesh of the 3D groundwater model.

While the utility provides a quick estimate of FoS_{piping} at each of the boundary-face nodes of interest, more field data must be incorporated to compute FoS_{uplift} when non-pipeable surface materials (e.g., clay blanket) are present. Moreover, although this utility provides an effective way to identify the potential for initiation of internal erosion, additional considerations should be given to the likelihood that backward erosion piping would continue towards the reservoir and cause a breach. Additional soil mechanics information must be taken into account when completing internal erosion studies.

DEMONSTRATION EXAMPLE: A WASH123D model was developed within Reach 2 of the Herbert Hoover Dike (HHD) around Lake Okeechobee, Florida, to study the feasibility of a proposed Seepage Management Test Facility (SMTF) and a shallow cutoff wall alternative to mitigate seepage, as detailed in the HHD Flow Model Report (Pickett et al. 2013). Figure 4 depicts the typical embankment of the SMTF taken from construction plans. The HHD was built to prevent flooding of Lake Okeechobee and allowed for the development of the Everglades Agricultural Area (EAA). The SMTF includes a drainage system built into the downstream slope of the HHD and includes an inclined chimney drain to collect through-embankment seepage, a trench drain to intercept through-foundation seepage for pressure relief and a blanket drain to convey the seepage collected by the chimney and trench drains to the ditch. The shallow cutoff wall consists of an impermeable material installed along the HHD crest to inhibit horizontal seepage through the dike.

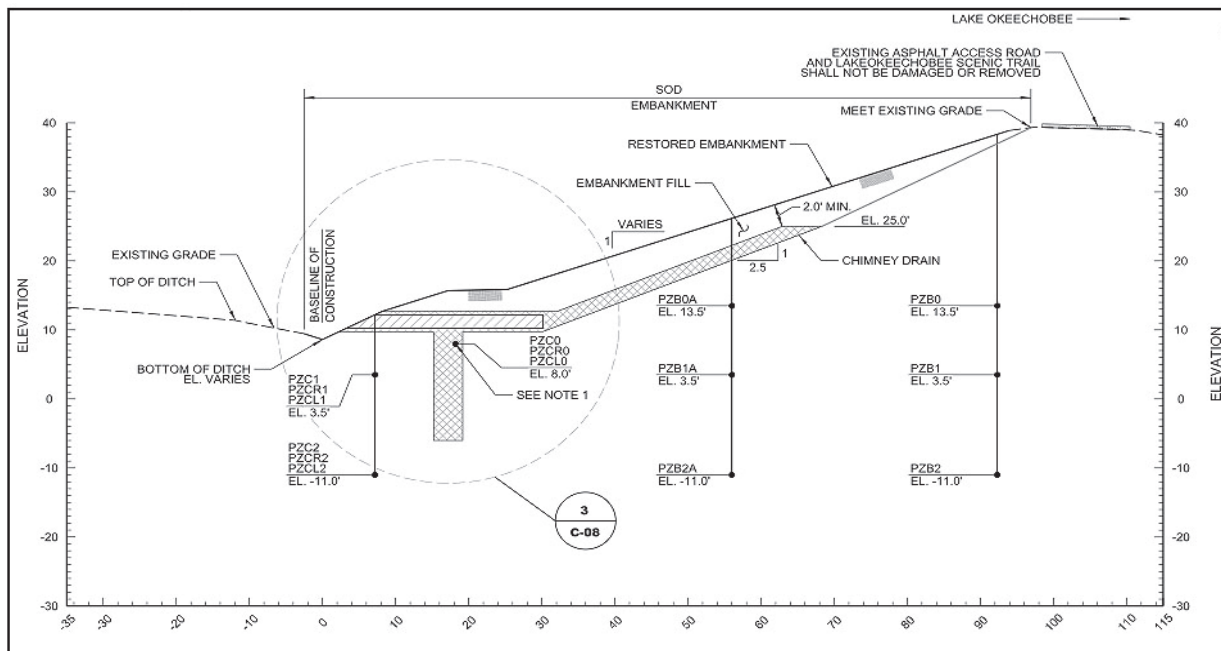


Figure 4. Typical embankment and instrumentation cross section of the SMTF from construction plans provided by the USACE, Jacksonville District.

Model Discretization. The model domain covers an area of 0.29 square miles and was discretized with 163,884 nodes and 570,940 elements. The mesh resolution varies to represent all of the SMTF and relevant surrounding features. This model consists of multiple element types with tetrahedrons on top of triangular prisms (Figure 5) to allow pinch out of material regions and additional resolution of the SMTF drain in the Z-axis direction.

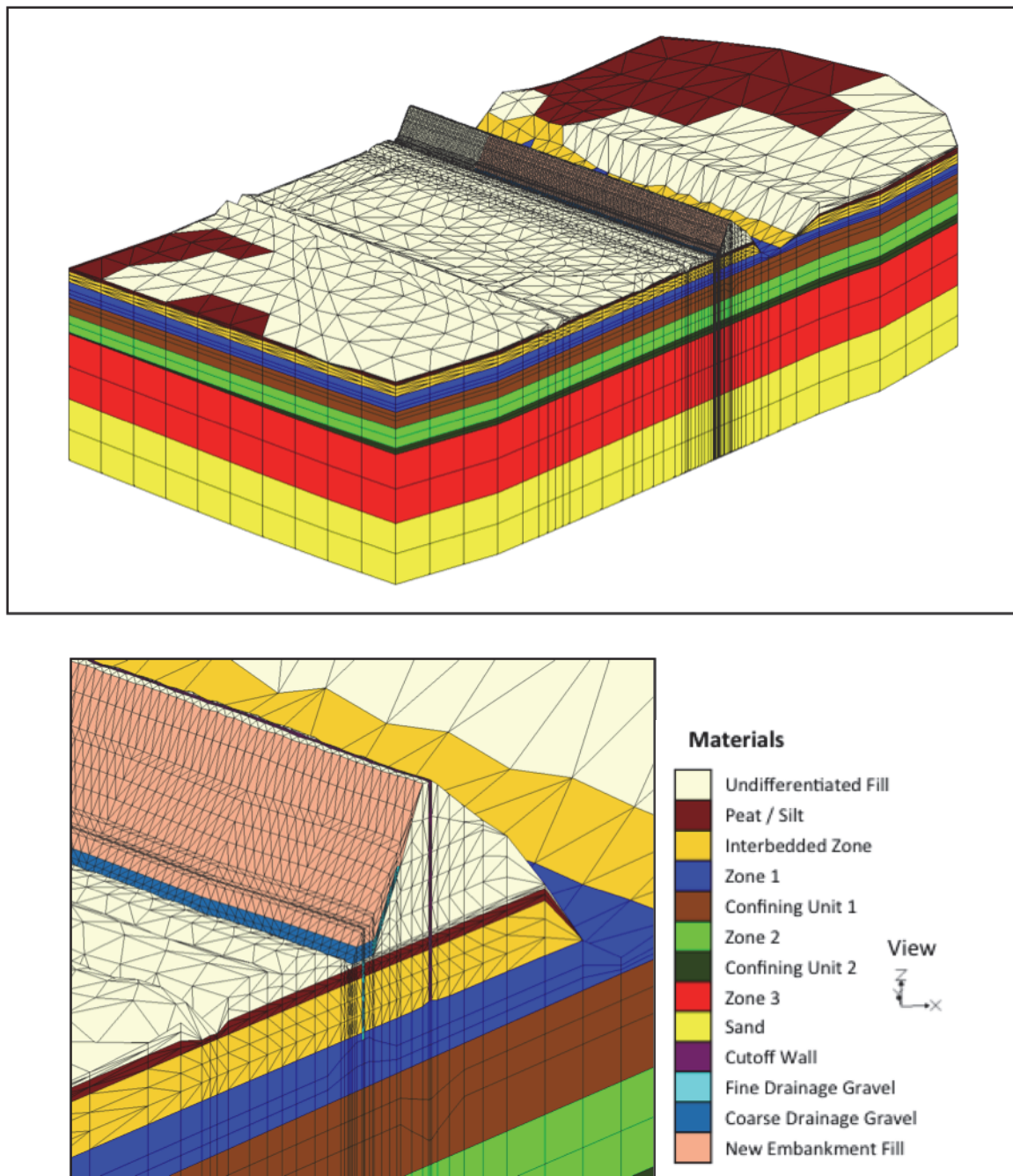


Figure 5. The WASH123D-SMTF model mesh with material assignments (full domain, top; close up of dike, bottom) shown vertically stretched (z-magnification = 5).

Geology and Configuration. As shown in Figure 6, the drainage system stretches three-quarters of the width of the model domain and two-thirds of the landside HHD face (from toe ditch to crest) with the upper chimney resting in the Undifferentiated Fill, covered by New Embankment Fill, and the lower chimney cutting through the Peat/Silt and Interbedded Zone regions into Zone 1. The New Embankment Fill overlays a larger area than the Drainage Gravels due to construction grading (Figure 4) and is assumed to retain original Undifferentiated Fill

material properties from proper compaction (materials are distinguishable only by name). The drain face is approximately 3 ft above the toe ditch thalweg that incises into the Peat/Silt region. Figure 6 also shows the shallow cutoff wall configuration, which extends the entire width of the domain and terminates at the interface of the Interbedded Zone and Zone 1. Figure 7 presents the four configurations considered in the study: existing, shallow cutoff wall, SMTF drainage system (hereafter referred to as just *drain*), and shallow cutoff wall with drain.

Simulation Results. Five sets of boundary conditions were considered in the study. However, only the set with an extremely high lake stage (i.e., 30 ft NAVD88) is presented herein for demonstration. Figure 8 shows the computed total head distributions associated with the four configurations from WASH123D. Figure 9 depicts the areal extents where the initiation of piping would likely occur due to high hydraulic gradients according to the FoS calculated using the utility code. The FoS analysis was conducted on the entire surface nodes of the model. To filter the results, four values (1, 1.25, 1.5, and 2) were used as screening criteria. It was assumed that areas with FoS values > 2 would always be stable.

Focusing on the Peat/Silt material region of the toe ditch, the shallow cutoff wall provides nearly no protection because it does not regulate flow into the toe ditch. It is effective, though, in increasing the FoS on the embankment surface (not shown in Figure 9 since $\text{FoS} > 2$). Conversely, the drain effectively reduces the hydraulic gradient at the toe ditch bottom by diverting the flow and increasing the FoS as a result. The combination of the shallow cutoff wall and drain had negligible gain from the drain alone. This result is better seen in Tables 1 and 2.

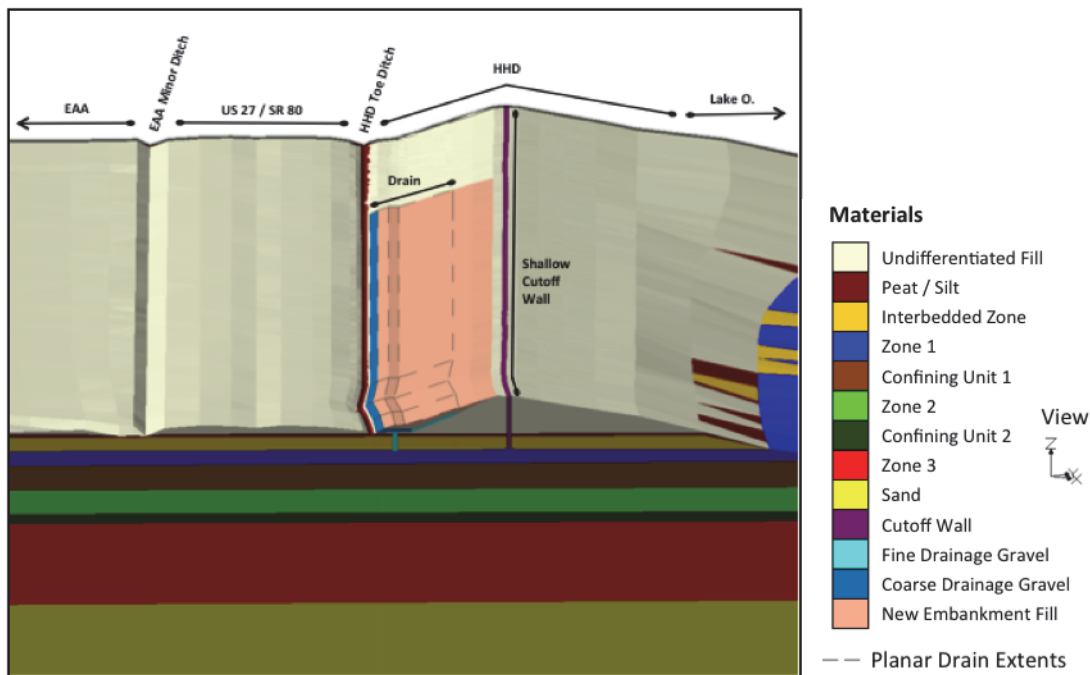


Figure 6. The WASH123D-SMTF model geology, shallow cutoff wall, and drain regions.

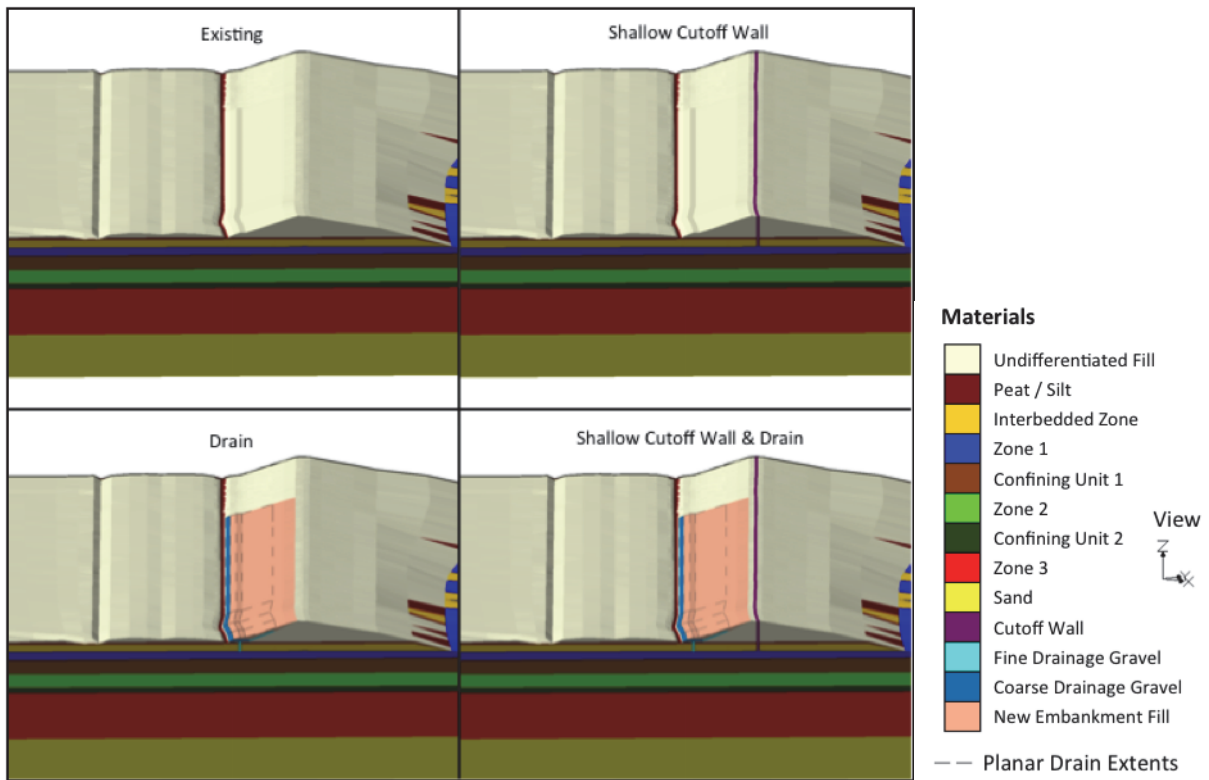


Figure 7. The WASH123D-SMTF model configurations.

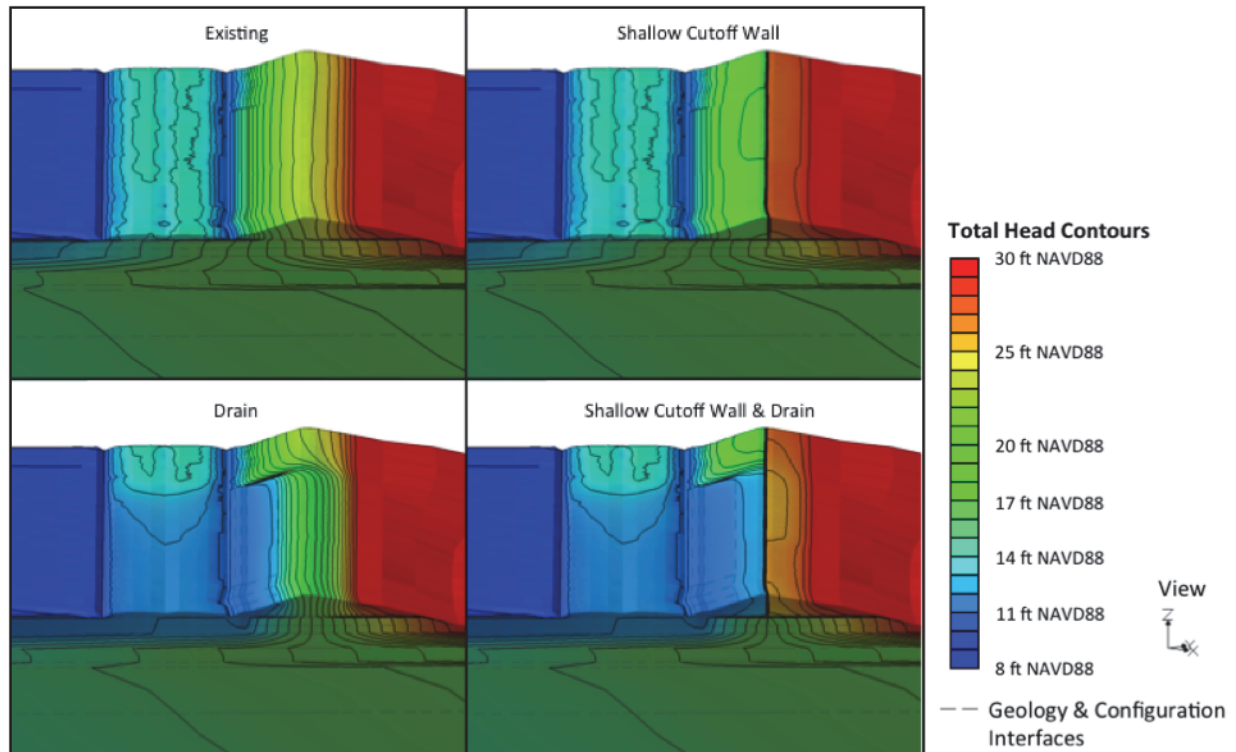


Figure 8. The WASH123D-SMTF model total head distribution along the embankment.

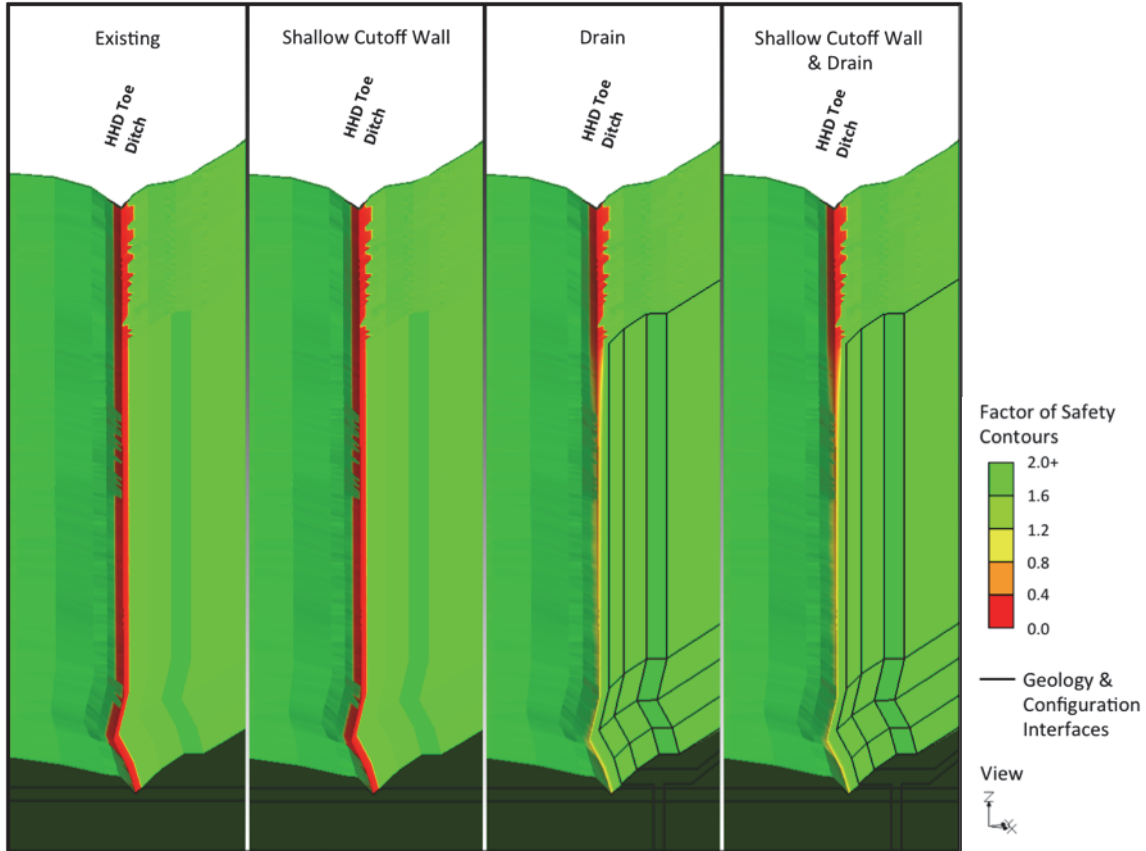


Figure 9. The WASH123D-SMTF model FoS distribution along the embankment (close up of HHD toe ditch).

Table 1. FoS Distribution on WASH123D-SMTF Model Surface Nodes				
Value	Number of Occurrences (per model configuration)			
	Existing	Shallow Cutoff Wall	Drain	Shallow Cutoff Wall & Drain
FoS < 1.00	681	681	423	422
1.00 ≤ FoS < 1.25	7	7	20	20
1.25 ≤ FoS < 1.50	0	0	47	43
1.50 ≤ FoS < 2.00	2	2	101	99
2.00 ≤ FoS	1,958	1,810	1,167	1,120
Unquantifiable	3,902	4,050	4,792	4,846

Note: FoS values were calculated at all quantifiable surface locations where hydraulic gradient caused water to exit the ground. Surface mesh of 6,550 total nodes, HHD toe ditch thalweg consists of 201 nodes with an approximately 10 ft spacing, and EAA minor ditch consists of 68 nodes with an approximately 30 ft spacing.

Table 2. Comparison of Average FoS of WASH123D-SMTF Model Configurations		
Configuration	Average FoS	Average FoS Increase % (from Existing)
Existing	0.215	---
Shallow Cutoff Wall	0.219	1.7%
Drain	0.755	250.7%
Shallow Cutoff Wall & Drain	0.749	247.7%

Note: Only surface locations with FoS between 0 and 2 were used to calculate average values. Change in percentage values are the increase in FoS caused by the proposed configuration compared to the existing configuration

Table 1 lists the number of surface locations within various FoS criteria ranges. Table 2 lists an overall average FoS, when considering just surface locations with $FoS < 2$, and percent change in the overall average FoS comparing the configurations to the respective existing condition of each boundary condition set. These *occurring failure* results rely on a regional geology conceptual model that simplifies heterogeneity local to the HHD and underestimates existing conditions preventing failure, such as vegetation. However, note that the change of FoS due to controlling seepage is a legitimate and usable result.

SUMMARY: A utility code was developed to compute FoS_{piping} at boundary-face nodes using the computed heads from 3D groundwater simulations. The utility code computes exit gradients and uses a simple equation (Equation 14) to estimate the FoS_{piping} at locations on a sloped boundary face based on both the vertical FoS (Equation 12) and the horizontal FoS (Equation 13). A groundwater model developed for an SMTF feasibility study was employed for demonstration. The model accounts for a drainage system as well as a cutoff wall. Four configurations were compared to help identify effective components for seepage management. Note that the FoS results of the model rely on a regional geology conceptual model that simplifies heterogeneity local to the HHD. Future evaluations of the WASH123D-SMTF model would benefit from the incorporation of epistemic uncertainty. Additional knowledge and data should necessitate increasing the mesh resolution that would refine the FoS analysis. For future improvement, Equation 11 can be incorporated into the utility to compute FoS_{uplift} for nonpipeable surface materials.

ADDITIONAL INFORMATION: This work was completed for an HHD groundwater modeling project, funded by the U.S. Army Corps of Engineers (USACE), Jacksonville District. Dr. Stacy E. Howington of the U.S. Army Engineer Research and Development Center (ERDC), Coastal and Hydraulics Laboratory (CHL); Laura D. Bittner, P.E., Chief of Hydrology, Hydraulics, and Coastal Branch, of the USACE, Philadelphia District; and Bradley Cox of the USACE, Jacksonville District, reviewed this technical note and provided valuable comments. For additional information, contact Hwai-Ping (Pearce) Cheng, ERDC/CHL, 3909 Halls Ferry Road, Vicksburg, MS 39180, at 601-634-3699 or e-mail: Hwai-Ping.Cheng@usace.army.mil. This CHETN should be cited as follows:

Cheng, H.-P., K. D. Winters, S. M. England, and R. E. Pickett. 2014. *Factor of safety analysis using 3D groundwater simulation results*. ERDC/CHL CHETN-XI-2. Vicksburg, MS: U.S. Army Engineer Research and Development Center.

An electronic copy of this CHETN is available from <http://chl.erdcl.usace.army.mil/chetn>.

REFERENCES

- Al-Hussaini, M. M., R. E. Wahl, J. F. Peters, and T. L. Holmes. 1997. *Seepage and stability analysis of Herbert Hoover Dike*. Technical Report GL-97-2. Vicksburg, MS: USACE Waterways Experiment Station, 61–63.
- Davis, J. R., E. D. Guy, and R. L. Nettles. 2009. Herbert Hoover Dike seepage remedial design concepts. In *Proceedings, 29th Annual U.S. Society on Dams Conference, 20-24 April, Nashville, Tennessee*, 685–706. Denver, CO: U.S. Society on Dams.
- Duncan, J. M. 2000. Factors of safety and reliability in geotechnical engineering. *Journal of Geotechnical and Geoenvironmental Engineering* 126(4): 307–316.
- U.S. Army Corps of Engineers (USACE), Jacksonville District. 2008. *Herbert Hoover Dike loadings and factors of safety for use in seepage and stability analyses*. Memorandum for record. Jacksonville, FL: USACE, Jacksonville District.
- O’Leary, T., N. Vroman, C. Williams, and M. Pabst. 2013. Critical horizontal seepage gradient. *Journal of Dam Safety* 11(3): 33–42.
- Pickett, R. E., K. D. Winters, H.-P. Cheng, and S. M. England. 2013. *Herbert Hoover Dike (HHD) flow model*. Project Report submitted to SAJ. Vicksburg, MS: U. S. Army Engineer Research and Development Center.
- Yeh, G.-T., G. Huang, H.-P. Cheng, F. Zhang, H.-C. Lin, E. Edris, and D. Richards. 2006. A first-principle, physics-based watershed model: WASH123D. In *Watershed models*, ed. V. P. Singh and D. K. Frevert, 211–244. Boca Raton, FL: CRC Press, Taylor and Francis Group.

NOTE: *The contents of this technical note are not to be used for advertising, publication, or promotional purposes. Citation of trade names does not constitute an official endorsement or approval of the use of such products.*